DOI: 10.30511/pcdp.2025.2048230.1013 - ISSN: 3060-8376 - Vol 2(1), 2025

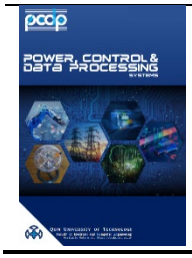

POWER, CONTROL AND DATA PROCESSING SYSTEMS

Available Online at: https://pcdp.qut.ac.ir/

Impact of Line Impedances and Loads on Compensation Capability of Electric Springs

ARTICLE INFO

Article Type
Original Research

Authors
M. Shademan[1]
A. Jalilian[2, *]

Department of electrical engineering, Iran University of Science and Technology, Tehran, Iran, mohamadmahdishademan@gmail.com
[2] Department of Electrical engineering, Iran University of Science and Technology, Tehran, Iran, jalilian@iust.ac.ir

*** *Correspondence***
Address: Department of electrical engineering, Iran University of Science and Technology, Heidarkhani Street,
Tehran, Iran. Postal Code: 71551313.
Phone: +982173225607
Fax: -
jalilian@iust.ac.ir

Article History
Received: December 15, 2024
Accepted: February 07, 2024
ePublished: March 01, 2025

ABSTRACT

The electric spring is used as a demand side management device in the smart grid. Electric springs can be effective in applications such as voltage and power regulation, three-phase load balancing, harmonics compensation, and improve voltage stability by utilizing inverters and mounting on the consumer side. On the other hand, the increasing expansion of renewable energies, the emergence of micro-grids, and electric vehicles are exacerbating power quality issues such as undervoltage, overvoltage, unbalanced loads, and harmonics in the power distribution grid. Therefore, electric springs can provide appropriate voltage quality for critical loads (E.g., building security systems, computers, and digital systems) by connecting series to non-critical loads (E.g., electric water heater, washing machine, and air conditioner) and using different control methods. In this paper, the effect of changes in the magnitude and angle of each line impedance, noncritical load, and critical load on the ability of voltage compensating of electric spring is investigated. For this purpose, two operating modes of overvoltage and undervoltage have been considered to obtain the compensation limits of electric spring. Finally, in this paper, an allowable range for the magnitude and angle of each impedance is proposed, in which the electric spring can compensate for voltage fluctuations without instability.

Keywords: Smart Load; Electric Spring; Power Quality; Voltage Regulation, Demand Side Management.

1 Introduction

With the increasing expansion of local renewable sources (such as solar panels and wind turbines), the distribution networks are moving away from the centralized mode and towards dispersed productions and islanding of microgrids. Also, the emergence of electric cars and their charging and discharging issues are among the other things that we are very connected with today. The mentioned cases cause fluctuations in production and consumption, which causes power quality issues such as voltage shortage, overvoltage, frequency fluctuation and load imbalance. On the other hand, the widespread use of power electronics such as converters, both in the production and consumption sectors, has caused harmonics in microgrids. Electric springs (ESs) as devices on the consumer side are a solution to solve many of these problems. The ES consists of an inverter, a dc source, a passive filter and a control system, which is used both as a single phase and as a three phase, and in series with a non-critical load (NCL), such as an electric water heater, washing machine, and air conditioning system. ESs are installed to provide adequate voltage quality for critical loads (CLs), such as building security system, computers and digital systems, placed in parallel with them. Also, the set of NCLs and ES that are placed in series with each other is called smart load (SL). SLs have the ability to follow fluctuations in power production by renewable sources, that's why the are suitable tools for demand response in smart networks.

ESs were initially introduced as tools for real-time voltage and power stability by Rui in [1]. In [2], a control method for voltage stabilization through reactive power control by ES is presented. In [3], the dynamic model of the ES for voltage and frequency control has been investigated. In [4], it describes the drop control method for the parallel operation of ESs distributed in the network to stabilize the power network through reactive power control. In [5], the collective control method for the operation of parallel and distributed ESs in the network for voltage and frequency control has been investigated and its results have been compared with the droop control method. Also, a control method based on the difference between the voltage angle of the network source and the voltage of the sensitive load (δ control) is presented in [6]. In [7], the control methods to adjust the voltage through controlling the active and reactive power of the ES are presented simultaneously to form the 2nd generation ESs. The 3rd generation ESs that use solar panels instead of batteries are presented in [8]. Also, the use of back-to-back converters that feed from the network itself is introduced in [9]. In [10], authors used an ES to remove the negative and zero sequences in an unbalanced three-phase network. In [11], a control system has been added to the previous methods to reduce the harmonics caused by the network source voltage on CLs. The use of ESs is also used in DC networks, the introduction of the structure and control method of this type of compensators is given in [12]. The modeling of a thermal storage system as an NCL connected to an ES is given in [13] to deal with the problem of imbalance between power generation and consumption with the control method presented in it. In [14], a control method based on an ES is proposed to improve resilience in microgrid. Also, in order to improve the flexibility of the islanded microgrid, a control method based on an ES has been presented in [15].

The difference between ES and other voltage control devices, such as SSSC, STATCOM, UPFC and APF, is that all these devices do not distinguish between CL and NCL loads. Also, the ES is an innovation on the consumer side, which is exploited by being distributed among consumers and takes advantage of decentralized control. Meanwhile, the devices mentioned above are used on the network side and in a sensitive bus and require centralized control. Therefore, they need telecommunication systems and infrastructure, but the ES does not need telecommunication systems. It has also been proven in [16] that the use of a group of ESs has less reactive power than a STATCOM. The comparison of these tools is shown in Table. 1.

Table 1: Comparison between voltage control devices [16].

Types of compensators	How to connect	Control method	Need a transformer
Electric spring	series	Decentralized	does not have
SSSC	series	Centralized	has
STATCOM	parallel	Centralized	has
UPFC	series and parallel	Centralized	has
APF	Mostly parallel	Centralized	has

In all these articles, the performance of the ES and possible control systems have been discussed, but less attention has been paid to the effect of each of the impedances in the circuit on the compensation performance of the ES. For example, in the article [17], the effect of line impedance on the compensation capability of the ES has been investigated, but the effect of other impedances such as CL and NCL has not been mentioned.

In this article, we investigate the effect of each line impedance, NCL and CL on the operation of voltage adjustment by ES and its compensation range. In this way, by examining different impedances, both in terms of magnitude and angle, the ability of the ES will be more understandable in terms of different dimensions, such as the level of power consumption of the load, the type of loads, and the type of network.

For this reason, two modes are considered:

- Fixed angle mode and variable magnitude
- Fixed magnitude and variable angle mode

In the first case, by keeping the angle of each of these three impedances constant, we change the magnitude of the impedances to understand the effect of changing the magnitude of the impedances on the compensation range of the ES. Also, in the second case, the magnitude of each of the impedances is assumed to be constant in order to understand the effect of changing the angle of the impedances on the compensation range of the ES. On the other hand, the compensation range of the ES is limited to a maximum

undervoltage compensation and a maximum overvoltage compensation. Therefore, in this article, 12 possible modes will be examined in order to get a better understanding of the existing system.

In this regard, in section 2, the principle of operation of the ES and the description of the used control system will be discussed, and also the physical relations governing the circuit will be explained. In part 3, we will simulate the ES in Matlab 2019b software, and the effect of the impedances in the network on the ability to compensate the ES in overvoltage and undervoltage states will be discussed. Finally, in section 4, we will review the conclusions from the outputs.

2 Principles of ES operation

The ES consists of an inverter, dc power supply, and filter. The ES is installed in series with NCLs (such as refrigerator, air conditioning system and electric water heater) and the set of ES and NCL is called SL. SL is placed in parallel with CL (such as building security system, computers and digital systems). Also, the set of CL and SL are connected to renewable energy sources (such as solar energy, wind energy) in a microgrid through a line impedance, which is shown in Figure. 1.

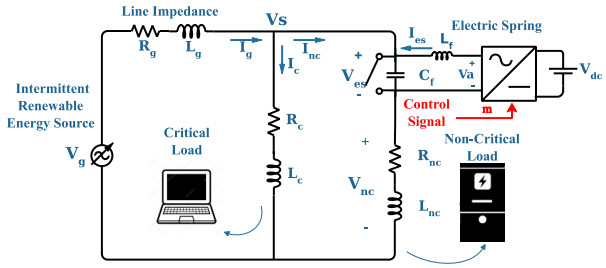

Figure 1: Application of ES in the circuit [7].

In the condition that the bypass switch *s* is closed, the ES is short-circuited and it is like it does not exist in the circuit, so the NCL is directly connected to the mains. In this case, due to the use of renewable resources in the network, if not properly adjusted, the point of common coupling (PCC) voltage fluctuates wildly. This voltage fluctuation causes destructive effects in CLs, but NCLs are more resistant to these changes.

When the *s* key is open, the ES enters the circuit. The ES can be modeled in terms of a circuit with a dependent voltage source so that the magnitude and angle of the voltage produced by the ES can be controlled by switching the semiconductor elements in the inverter. Therefore, the voltage generated by the ES can change the PCC voltage in such a way that when the network voltage drops, the ES increases the voltage of the CL and when the network voltage increases, it causes the voltage in the sensitive load to decrease. In this way, by controlling the inverter, the voltage of the CL can be kept constant on its rated value.

Switching control in the inverter can be done with the help of a closed loop control system. For this purpose, various control systems have been presented, which are shown in articles [2-7].

The control system used in this article for simulation is shown in Figure 2.

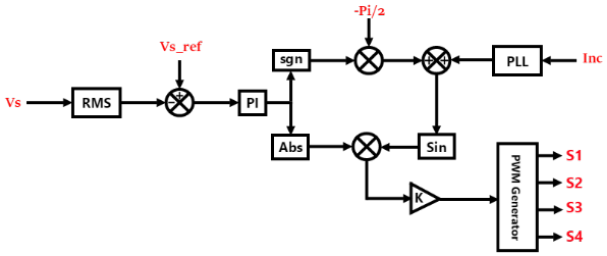

Figure 2: The used control system [2].

According to the control system, the ES will produce its voltage in such a way that its voltage is perpendicular to the current passing through the NCL and also to itself. Also, the magnitude of the generated voltage depends on the difference between the effective voltage value of the CL and the nominal value of the CL. Because in this system, feedback is taken directly from the voltage of the CL and after comparing it with its nominal value, it is connected to a PI controller. In this way, the ES only adjusts the voltage of the CL to the nominal value through reactive power control.

Also, due to the use of the battery as an energy source in the ES, the dc link voltage is considered constant and there is no need for a control loop to keep the dc link voltage constant. But if a capacitor is used instead of a battery as in [2] article, the DC link voltage must be set to the appropriate value through a PI controller, in which case the ES will be limited to compensation through reactive power.

It should be noted that the PI controller coefficients are set based on the Ziegler-Nichols method. In this method, assuming that there is no integral coefficient, we increase the proportional coefficient to such an extent that the response of this controller becomes completely oscillating and infinite around the answer. The obtained coefficient is called critical coefficient and is denoted by (K_{cr}). We also measure the period of oscillation of the answer and name it (T_{cr}). Based on this method, P and I coefficients are selected as $0.45K_{cr}$ and $T_{cr}/1.2$, respectively. With this method, which has an empirical basis, the response of the controller can be adjusted to an optimal level.

The ES to adjust the voltage has two modes:

A) Undervoltage mode:

In this case, the error entered into the PI controller is positive and the output of the sgn block will be positive in this case, which after multiplying by the constant value of π/2, will decrease by 90 degrees from the NCL current angle to form the ES voltage angle, working in mere capacitor mode. The operation diagram of the ES in the state of voltage deficiency is shown in Figure. 3.

B) Overvoltage mode:

In this case, the error input to the PI controller is negative and the output of the *sgn* block will be negative in this case, which after multiplying by the constant value of π/2, adds 90 degrees

to the NCL current angle to form the ES voltage angle, working in mere inductive mode. The operation diagram of the ES in overvoltage mode is shown in Figure. 4.

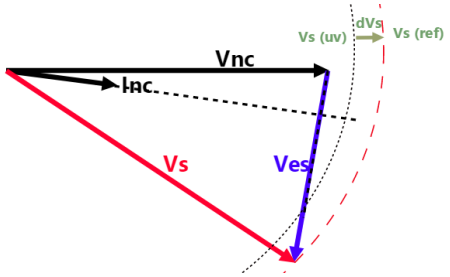

Figure 3: Undervoltage mode [2].

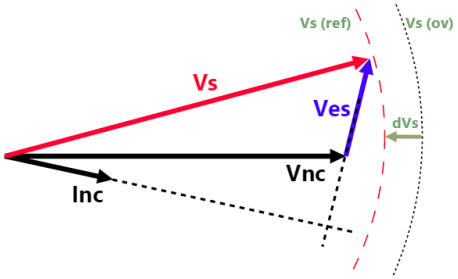

Figure 4: Overvoltage mode [2].

According to Figure. 1, the main circuit equations governing this circuit are as follows:

$$\overrightarrow{v_s} = \overrightarrow{v_{nc}} + \overrightarrow{v_{es}} \quad \text{Eq1}$$

$$\overrightarrow{i_g} = \overrightarrow{i_{nc}} + \overrightarrow{i_c} \quad \text{Eq2}$$

$$\overrightarrow{i_g} = \frac{\overrightarrow{v_g} - \overrightarrow{v_s}}{Z_g} \quad \text{Eq3}$$

$$\overrightarrow{i_{nc}} = \frac{\overrightarrow{v_s} - \overrightarrow{v_{es}}}{Z_{nc}} \quad \text{Eq4}$$

$$\overrightarrow{i_c} = \frac{\overrightarrow{v_s}}{Z_c} \quad \text{Eq5}$$

In these equations, V_s, V_{nc}, and V_{es} are equal to the network voltage, NCL voltage, and ES voltage, respectively; i_g, i_{nc} and i_c are respectively equal to the line current, NCL current (or ES current), and CL current; Also, Z_g, Z_{nc}, and Z_c are equal to line impedance, NCL impedance, and CL impedance, respectively. Assuming that we consider the ES as a capacitor in the state of undervoltage and as an inductive in the state of overvoltage:

$$\begin{cases} Z_c = |Z_c|\angle\varphi_c \\ Z_{nc} = |Z_{nc}|\angle\varphi_{nc} \\ Z_g = |Z_g|\angle\varphi_g \\ Z_{es} = \mp jX_{es} \end{cases} \quad \text{Eq6}$$

In permanent mode, the ES compensates the voltage of the CL and brings it to its nominal value. Therefore, by considering the nominal value of the CL voltage as the base value, the relationships can be considered as per-unit (PU) ($\overrightarrow{V_s^{pu}} = 1\angle 0$). Now, according to equations 1 to 6, equations 7 to 9 are obtained as follows:

$$\overrightarrow{i_c^{pu}} = \frac{1}{Z_c} = \frac{1}{|Z_c|}\angle -\varphi_c = \frac{Cos\,\varphi_c}{|Z_c|} - j\frac{Sin\,\varphi_c}{|Z_c|} \quad \text{Eq7}$$

$$\overrightarrow{i_{nc}^{pu}} = \frac{1}{Z_{nc} - jX_{es}} = \frac{|Z_{nc}|\,Cos\,\varphi_{nc} - j(|Z_{nc}|\,Sin\,\varphi_{nc} - X_{es})}{|Z_{nc}|^2 + {X_{es}}^2 - 2|Z_{nc}|X_{es}\,Sin\,\varphi_{nc}} \quad \text{Eq8}$$

$$\overrightarrow{i_g^{pu}} = \left\{\frac{Cos\,\varphi_c}{|Z_c|} + \frac{|Z_{nc}|\,Cos\,\varphi_{nc}}{|Z_{nc}|^2 + {X_{es}}^2 - 2|Z_{nc}|X_{es}\,Sin\,\varphi_{nc}}\right\} - j\left\{\frac{Sin\,\varphi_c}{|Z_c|} + \frac{(|Z_{nc}|\,Sin\,\varphi_{nc} - X_{es})}{|Z_{nc}|^2 + {X_{es}}^2 - 2|Z_{nc}|X_{es}\,Sin\,\varphi_{nc}}\right\} \quad \text{Eq9}$$

Now assuming ($\overrightarrow{V_g^{pu}} = |V_g^{pu}|\angle\delta$) and writing the KVL equation in the line impedance branch, we have:

$$\overrightarrow{i_g^{pu}} = \frac{|V_g^{pu}|\angle\delta - 1\angle 0}{|Z_g|\angle\varphi_g} = \left\{\frac{|V_g^{pu}|}{|Z_g|}Cos(\delta - \varphi_g) - \frac{Cos\,\varphi_g}{|Z_g|}\right\} + j\left\{\frac{|V_g^{pu}|}{|Z_g|}Sin(\delta - \varphi_g) + \frac{Sin\,\varphi_g}{|Z_g|}\right\} \quad \text{Eq10}$$

Now, by equating equations (9) and (10), the following two equations are obtained based on the real and imaginary parts:

$$\frac{|V_g^{pu}|}{|Z_g|}Cos(\varphi_g - \delta) = \frac{Cos\,\varphi_g}{|Z_g|} + \frac{Cos\,\varphi_c}{|Z_c|} + \frac{|Z_{nc}|\,Cos\,\varphi_{nc}}{|Z_{nc}|^2 + {X_{es}}^2 - 2|Z_{nc}|X_{es}\,Sin\,\varphi_{nc}} \quad \text{Eq11}$$

$$\frac{|V_g^{pu}|}{|Z_g|}Sin(\varphi_g - \delta) = \frac{Sin\,\varphi_g}{|Z_g|} + \frac{Sin\,\varphi_c}{|Z_c|} + \frac{(|Z_{nc}|\,Sin\,\varphi_{nc} - X_{es})}{|Z_{nc}|^2 + {X_{es}}^2 - 2|Z_{nc}|X_{es}\,Sin\,\varphi_{nc}} \quad \text{Eq12}$$

In equation 11 and 12, there are two unknown variables. Therefore, we will have two equations and two unknown variables. In other words, there is an expression for each value of one, based on which the angle is obtained. By solving this equation, it is calculated as follows:

$$X_{es} = |Z_{nc}|\,Sin\,\varphi_{nc} - \frac{\beta}{2\alpha} \pm \sqrt{\frac{\gamma}{\alpha} - |Z_{nc}|^2\,Cos^2\,\varphi_{nc} + \frac{\beta^2}{4\alpha^2} - \frac{\beta}{\alpha}|Z_{nc}|\,Sin\,\varphi_{nc}} \quad \text{Eq13}$$

$$\delta = \varphi_g - tan^{-1}\left\{\frac{\frac{Sin\,\varphi_g}{|Z_g|} + \frac{Sin\,\varphi_c}{|Z_c|} + \frac{(|Z_{nc}|\,Sin\,\varphi_{nc} - X_{es})}{|Z_{nc}|^2 + {X_{es}}^2 - 2|Z_{nc}|X_{es}\,Sin\,\varphi_{nc}}}{\frac{Cos\,\varphi_g}{|Z_g|} + \frac{Cos\,\varphi_c}{|Z_c|} + \frac{|Z_{nc}|\,Cos\,\varphi_{nc}}{|Z_{nc}|^2 + {X_{es}}^2 - 2|Z_{nc}|X_{es}\,Sin\,\varphi_{nc}}}\right\} \quad \text{Eq14}$$

In the above equations, because we assumed the ES as a capacitor and took into account its sign, we accept the positive sign of X_{es} as the answer. Also, the values of α, β, and γ are obtained as follows:

$$\alpha = |V_g^{pu}|^2 - \left(\frac{|Z_g|}{|Z_c|}\right)^2 - 2\frac{|Z_g|}{|Z_c|}Cos(\varphi_g - \varphi_c) - 1 \quad \text{Eq15}$$

$$\beta = 2|Z_g|(Sin\,\varphi_g + \frac{|Z_g|}{|Z_c|}Sin\,\varphi_c) \quad \text{Eq16}$$

$$\gamma = |Z_g|^2(1 + 2\frac{|Z_{nc}|}{|Z_c|}Cos(\varphi_{nc} - \varphi_c)) + 2|Z_g||Z_{nc}|\,Cos(\varphi_{nc} - \varphi_g) \quad \text{Eq17}$$

Due to stability issues, it should be considered that the active and reactive tone does not flow from the consumer side to the network side. Therefore, the following restrictions should be considered:

$$\delta > 0 \quad \text{Eq18}$$

$$|V_g^{pu}| \geq 1 \quad \text{Eq19}$$

Also, to calculate the percentage of voltage drop or overvoltage, the following relationship can be used:

$$\Delta V\% = \frac{V_s^b - V_{s-ref}}{V_{s-ref}} \times 100 \quad \text{Eq20}$$

which in the above relationship is the effective value of the CL voltage before compensation and the effective value of the CL voltage after compensation or the nominal value of the CL voltage. The value can be calculated as follows by not considering the ES in the circuit:

$$V_s^b = \frac{V_g}{\left|1 + \frac{Z_g}{Z_{nc}} + \frac{Z_g}{Z_c}\right|} \qquad \text{Eq21}$$

3 Simulation and Results

In this part, the circuit system shown in Figure. 1 and its control system shown in Figure. 2 are simulated using Matlab Simulink 2019b software. The characteristics of said circuit are shown in Table. 2.

The performance results of the ES with the control system shown in Figure. 2, under constant impedances (both in terms of magnitude and angle) for two states of undervoltage and overvoltage, are shown in Figures 5 and 6. It is given that they correspond to Figures 3 and 4, respectively.

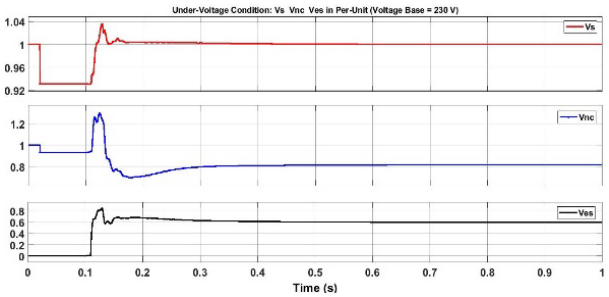

Figure 5: Compensating undervoltage by an ES in terms of per-unit (nominal voltage 230 V).

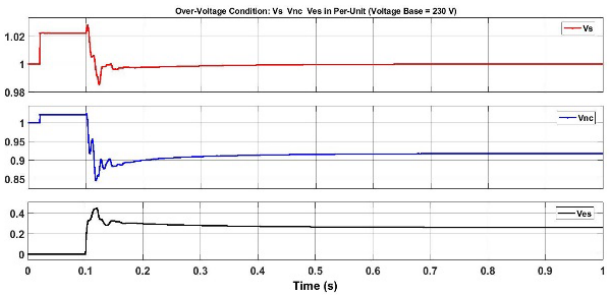

Figure 6: Compensating overvoltage by an ES in terms of per-unit (nominal voltage 230 V).

In the following, we consider the network voltage in two states of undervoltage and overvoltage. We will see that the ES has the ability to compensate for undervoltage and overvoltage to a certain extent. By changing the magnitude and angle of each of the line impedances, CL and NCL, the compensation limits of the ES for undervoltage and overvoltage changes, which is reviewed in this section. In this system, the nominal voltage selected for the CL or the SL is 230 volts (RMS). Also, the loads are considered as ohmic-inductive, so they have a lag power factor.

In order to measure the maximum overvoltage and the maximum undervoltage that can be compensated by the ES, we increase and decrease the grid voltage step by step, respectively. Any point of the network voltage where the ES was not capable of compensating for overvoltage or undervoltage is chosen as a border point and we calculate the voltage of the CL according to equation (21). Then, through equation (20), we measure the ability to compensate the maximum overvoltage or the maximum undervoltage by the ES and record it in the diagram.

Table 2: Circuit characteristics of the system and ES [7].

Circuit characteristics of the system	
Nominal voltage of CL: (RMS)	230 V
Network frequency	50 Hz
Line impedance	$Z_g = 0.1 + 0.7854j$
Sensitive load impedance	$Z_c = 11 + 11j$
Insensitive load impedance	Z_{nc}=6.11+0.44j
Circuit characteristics of electric spring	
Inverter structure	Full bridge-single phase
Switching frequency	20 kHz
Battery voltage (DC link)	400 V
The inductance of the low-pass filter inductor	1.92 mH
Capacitance of low pass filter	13.2 µF

3.1 Line Impedance

In this case, the impedance of the CL and the impedance of the NCL are considered constant, and the effect of the line impedance change on the compensation limits of the ES is evaluated. This work has been done once based on the magnitude change and once based on the line impedance angle change in the following.

A) Change in magnitude

In this case, we have kept the impedance angle of the line constant (82.75 degrees) and we change its magnitude from about zero to 8 ohms. The ability of the ES to support the maximum voltage drop and overvoltage as a percentage of the nominal voltage (230 V) is shown in Figure. 7 and Figure. 8, respectively.

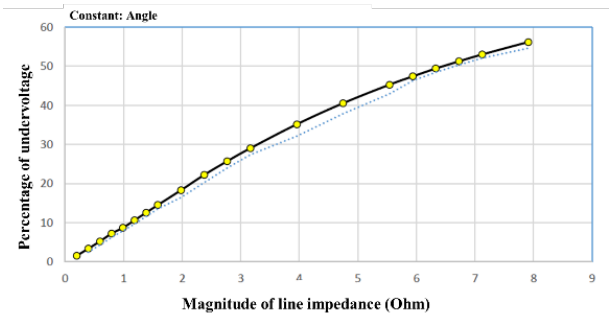

Figure 7: Undervoltage compensation by the ES in terms of per-unit when the magnitude of line impedance changes.

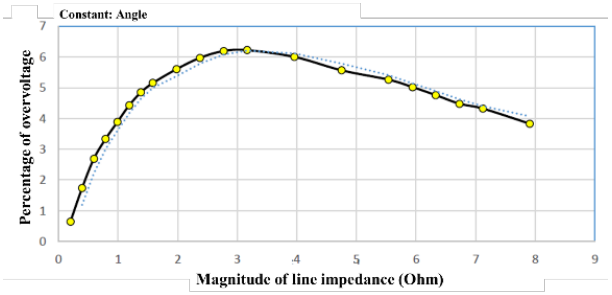

Figure 8: Overvoltage compensation by the ES in terms of per-unit when the magnitude of line impedance changes.

As can be seen, the more the line impedance increases, the more the ability to compensate for the maximum voltage deficiency increases. But the ability to compensate the maximum overvoltage has its maximum value at 3-ohm impedance (about 6%) and this ability decreases with values greater or less than 3 ohms.

b) Angle change

In this case, we have kept the impedance of the line constant (2.7 Ohms) and we change its angle from about zero to 90 degrees. The ability of the ES to support the maximum voltage drop and overvoltage as a percentage of the nominal voltage (230 V) is shown in Figures 9 and 10, respectively.

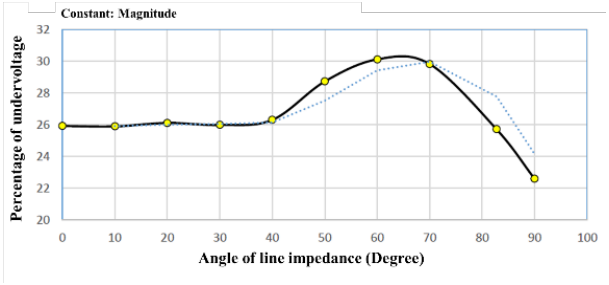

Figure 9: Undervoltage compensation by the ES in terms of per-unit when the angle of line impedance changes.

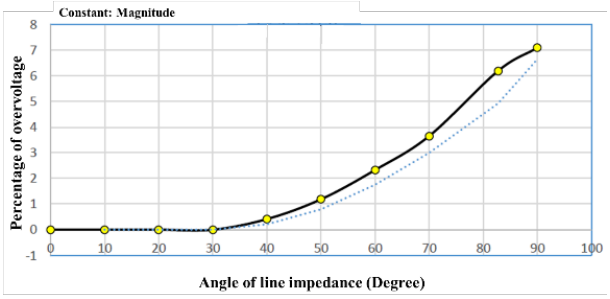

Figure 10: Overvoltage compensation by the ES in terms of per-unit when the angle of line impedance changes.

It can be seen from the Figure. 9 that up to an angle of 40 degrees, the ability to compensate the lack of voltage is almost constant. But after that, it has an increasing trend until the angle of 65 degrees, and then it completely decreases. It is also evident in Figure. 10 that the higher the impedance of the line becomes, the higher the ability to compensate for the maximum overvoltage.

3.2 Non-critical load

In this case, the impedance of the CL and the impedance of the line are considered constant, and the effect of changing the impedance of the NCL on the compensation limits of the ES is evaluated. This work has been done once based on the magnitude change and once based on the change of the NCL impedance angle in the following.

a) Change in magnitude:

In this case, we have kept the impedance angle of the insensitive load constant (4.12 degrees) and we change its magnitude from 2 to 9 ohms. The ability of the ES to support the maximum voltage drop and overvoltage as a percentage of the nominal voltage (230 V) is shown in Figure 11 and 12, respectively.

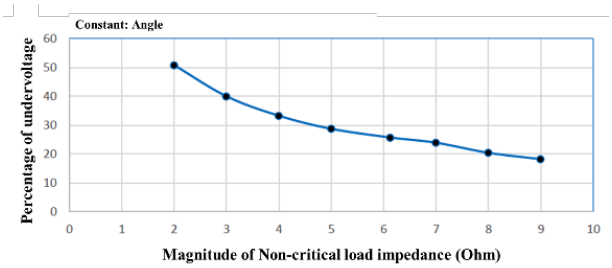

Figure 11: Undervoltage compensation by the ES in terms of per-unit when the magnitude of NCL changes.

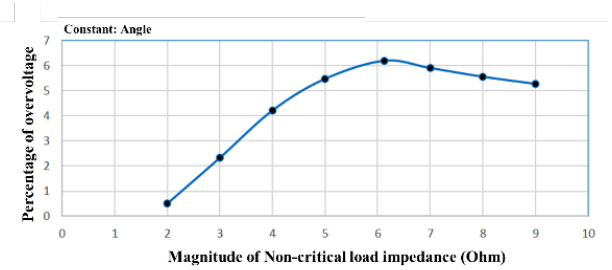

Figure 12: Overvoltage compensation by the ES in terms of per-unit when the magnitude of NCL changes.

As it is clear from Figure. 11, with the increase of the impedance of the NCL, the compensation percentage of the maximum voltage deficiency decreases. This means that by increasing the power consumption in the NCL, the ability to compensate by the ES in the state of undervoltage increases, which is desirable. On the other hand, in Figure. 12, it is clear that at the impedance of 6 ohms, the ability to compensate for the maximum overvoltage by the ES is at its maximum, and before and after this value, the graph takes a descending state. Therefore, the ability to compensate for the maximum overvoltage is a problem for high values in the apparent power of the NCL.

b) Angle change:

In this case, we have kept the magnitude of the NCL impedance constant (6.126 ohms) and we change its angle from about zero to 90 degrees. The ability of the ES to support the maximum undervoltage and overvoltage as a percentage of the nominal voltage (230 V) is shown in Figures 13 and 14, respectively.

It is clear from Figure. 13 that the more the NCL moves toward inductive condition, the greater the ability to compensate for the maximum voltage deficiency by the ES. But on the other hand, it can be seen from Figure. 14 that as the NCL becomes more inductive, the ability to compensate for the maximum overvoltage is less and even reaches zero percent. Therefore, values below 15 degrees are more reasonable for the NCL impedance angle.

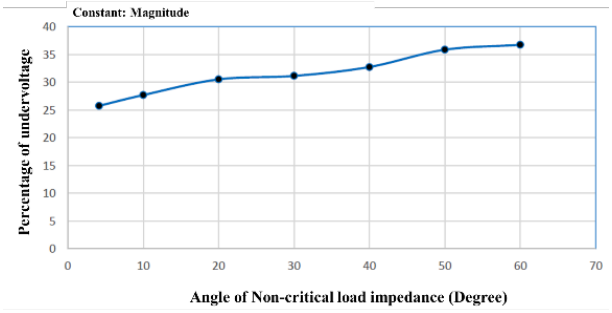

Figure 13: Undervoltage compensation by the ES in terms of per-unit when the angle of NCL changes.

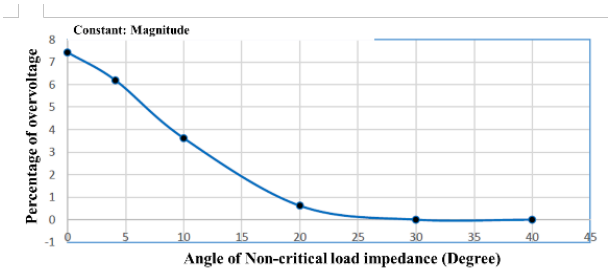

Figure 14: Overvoltage compensation by the ES in terms of per-unit when the angle of NCL changes.

3.3 Critical load

In this case, the impedance of the NCL and the impedance of the line are considered constant, and the effect of changing the impedance of the CL on the compensation limits of the ES is evaluated. This work has been done once based on the magnitude change and once based on the change of the impedance angle of the CL in the following.

a) Change in magnitude:

In this case, we have kept the impedance angle of the CL constant (45 degrees) and we change its magnitude from 2.83 to 28.3 ohms. The ability of the ES to support the maximum undervoltage and overvoltage as a percentage of the nominal voltage (230 V) is shown in Figures 15 and 16, respectively.

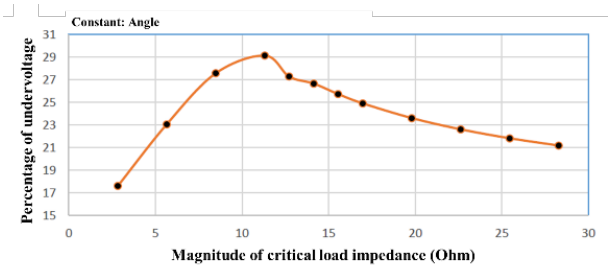

Figure 15: Undervoltage compensation by the ES in terms of per-unit when the magnitude of CL changes.

Figure. 15 shows that this diagram is at its maximum for an impedance of about 12 ohms, which is approximately equal to 29%, and for values greater than and less than 12 ohms, this diagram takes a downward state. On the other hand, it can be seen in Figure. 16 that the ability to compensate the maximum overvoltage increases with the increase in the impedance of the CL. Therefore, if the impedance of the CL is around 10 to 15 ohms, the performance of the ES will be favorable.

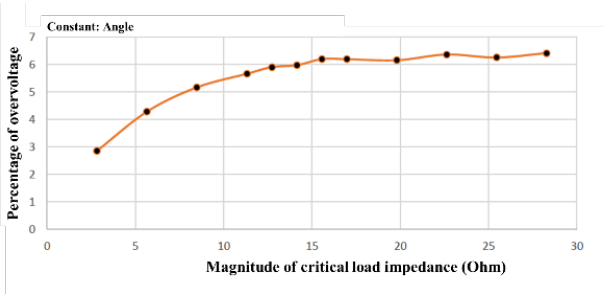

Figure 16: Overvoltage compensation by the ES in terms of per-unit when the magnitude of CL changes.

b) Angle change:

In this case, we have kept the impedance of the CL constant (15.5 ohms) and we change its angle from about zero to 90 degrees. The ability of the ES to support the maximum undervoltage and overvoltage as a percentage of the nominal voltage (230 V) is shown in Figures 15 and 16, respectively.

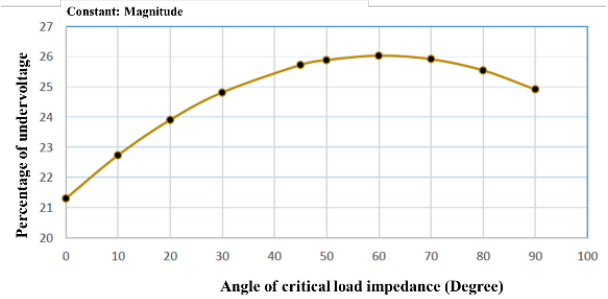

Figure 17: Undervoltage compensation by the ES in terms of per-unit when the angle of CL changes.

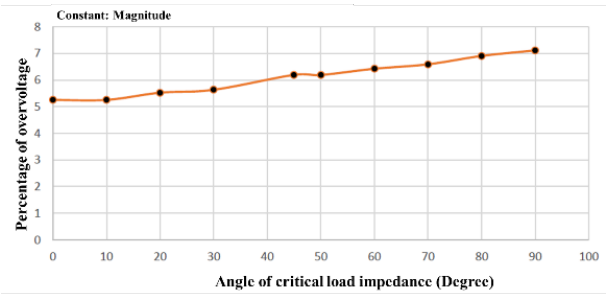

Figure 18: Overvoltage compensation by the ES in terms of per-unit when the angle of CL changes.

Figure. 17 shows that as the CL becomes more inductive, the ability to compensate for the maximum undervoltage by the ES first increases and then decreases. This diagram is at its maximum for CL with magnitude 15.5 and angle 60 degrees. It is also shown in Figure. 18 that the overvoltage compensation ability increases as the CL becomes more inductive.

4 Conclusion

ES is proposed to improve voltage and power stability in networks powered by renewable sources. Due to the fluctuating nature of such sources, it is possible that the voltage and power on the consumer side may suffer from undervoltage or overvoltage. In this article, the limitations of the ES in compensating overvoltage and undervoltage were discussed. In fact, the ES has the ability to compensate the undervoltage and the overvoltage caused by the network source to a certain extent. These limits depend on the magnitude and angle of line impedance, NCL impedance and CL impedance.

In this article, these three impedances have been tested in order to know the effect of changing the magnitude and angle of each of these impedances on the compensation range of the ES. For this reason, in section 3-1, by keeping the CL and NCL load constant, the impedance of the line has been changed. These changes have been made once as a fixed magnitude and once as a fixed angle. This procedure is also done for NCLs and CLs in sections 3-2 and 3-3, respectively.

Therefore, with the results obtained in this particular case, we can say:

• Increasing the magnitude of the impedance of the line improves the ability to compensate the undervoltage by the ES.

• Increasing the impedance angle of the line improves the overvoltage compensation capability by the ES.

• Reducing the magnitude of the impedance of the NCL improves the compensation of the undervoltage by the ES.

• Increasing the impedance angle of the NCL improves the ability to compensate the undervoltage by the ES.

• Increasing the impedance angle of the NCL strongly weakens the overvoltage compensation capability of the ES.

• Increasing the impedance of the CL improves the overvoltage compensation capability by the ES.

• Increasing the impedance angle of the CL improves the overvoltage compensation capability by the ES.

Disclosure of Potential Conflicts of Interest

The Authors declare that there is no conflict of interest

Reference

[1] S. Y. Hui, C. K. Lee, and F. F. Wu, “Electric springs - a new smart grid technology,” IEEE Transactions on Smart Grid, vol. 3, no. 3, pp. 1552–1561, Sept 2012.

[2] C. K. Lee, B. Chaudhuri, and S. Y. Hui, “Hardware and control implementation of electric springs for stabilizing future smart grid with intermittent renewable energy sources,” IEEE Journal of Emerging and Selected Topics in Power Electronics, vol. 1, no. 1 pp. 18–27, March 2013.

[3] N. R. Chaudhuri, C. K. Lee, B. Chaudhuri, and S. Y. R. Hui, “Dynamic modeling of electric springs,” IEEE Transactions on Smart Grid, vol. 5, no. 5, pp. 2450–2458, Sept 2014.

[4] C. K. Lee, N. R. Chaudhuri, B. Chaudhuri, and S. Y. R. Hui, “Droop control of distributed electric springs for stabilizing future power grid,” IEEE Transactions on Smart Grid, vol. 4, no. 3, pp. 1558–1566, Sept 2013.

[5] J. Chen, S. Yan, T. Yang, S. Tan and S. Y. Hui, "Practical Evaluation of Droop and Consensus Control of Distributed Electric Springs for Both Voltage and Frequency Regulation in Microgrid," in IEEE Transactions on Power Electronics, vol. 34, no. 7, pp. 6947-6959, July 2019.

[6] Qingsong Wang, Ming Cheng, Zhe Chen and Zheng Wang, "Steady-State Analysis of Electric Springs With a Novel δ Control," in IEEE Transactions on Power Electronics, vol. 30, no. 12, pp. 7159-7169, Dec. 2015.

[7] J. Soni and S. K. Panda, "Electric Spring for Voltage and Power Stability and Power Factor Correction," in IEEE Transactions on Industry Applications, vol. 53, no. 4, pp. 3871-3879, July-Aug. 2017.

[8] T. Yang, K. Mok, S. Ho, S. Tan, C. Lee and R. S. Y. Hui, "Use of Integrated Photovoltaic-Electric Spring System as a Power Balancer in Power Distribution Networks," in IEEE Transactions on Power Electronics, vol. 34, no. 6, pp. 5312-5324, June 2019.

[9] S. Yan et al., "Extending the Operating Range of Electric Spring Using Back-To-Back Converter: Hardware Implementation and Control," in IEEE Transactions on Power Electronics, vol. 32, no. 7, pp. 5171-5179, July 2017.

[10] K. Mok, S. Ho, S. Tan and S. Y. Hui, "A Comprehensive Analysis and Control Strategy for Nullifying Negative- and Zero-Sequence Currents in an Unbalanced Three-Phase Power System Using Electric Springs," in IEEE Transactions on Power Electronics, vol. 32, no. 10, pp. 7635-7650, Oct. 2017.

[11] Q. Wang, M. Cheng and Y. Jiang, "Harmonics Suppression for Critical Loads Using Electric Springs With Current-Source Inverters," in IEEE Journal of Emerging and Selected Topics in Power Electronics, vol. 4, no. 4, pp. 1362-1369, Dec. 2016.

[12] K. Mok, M. Wang, S. Tan and S. Y. R. Hui, "DC Electric Springs—A Technology for Stabilizing DC Power Distribution Systems," in IEEE Transactions on Power Electronics, vol. 32, no. 2, pp. 1088-1105, Feb. 2017.

[13] X. Luo, C. K. Lee, W. M. Ng, S. Yan, B. Chaudhuri and S. Y. R. Hui, "Use of Adaptive Thermal Storage System as Smart Load for Voltage Control and Demand Response," in IEEE Transactions on Smart Grid, vol. 8, no. 3, pp. 1231-1241, May 2017.

[14] L. Liang, Y. Hou, D. J. Hill and S. Y. R. Hui, "Enhancing Resilience of Microgrids With Electric Springs," in IEEE Transactions on Smart Grid, vol. 9, no. 3, pp. 2235-2247, May 2018.

[15] L. Liang, Y. Hou and D. J. Hill, "Enhancing Flexibility of an Islanded Microgrid With Electric Springs," in IEEE Transactions on Smart Grid, vol. 10, no. 1, pp. 899-909, Jan. 2019.

[16] Wang Q, Deng F, Cheng M, Buja G. The State of the Art of Topologies for Electric Springs. *Energies*. 2018; 11(7):1724.

[17] B. Sen, V. K. Kanakesh, J. Soni, C. D. Rodríguez-Gallegos and S. K. Panda, "Effect of line impedance on electric spring control," 2018 IEEE International Conference on Industrial Technology (ICIT), Lyon, 2018, pp. 1201-1206, doi: 10.1109/ICIT.2018.8352349.